Exploring the Magnetic Behavior of Nickel-Coordinated Pyrogallol[4]arene Nanocapsules

Harshita Kumari,[†] Cindi L. Dennis,[‡] Andrew V. Mossine,[†] Carol A. Deakyne,[†] and Jerry L. Atwood[†,*]

[†]Department of Chemistry, University of Missouri-Columbia, 601 South College Avenue, Columbia, Missouri 65211, United States, and [‡]Material Measurement Laboratory, National Institute of Standards and Technology, Gaithersburg, Maryland, United States

ABSTRACT

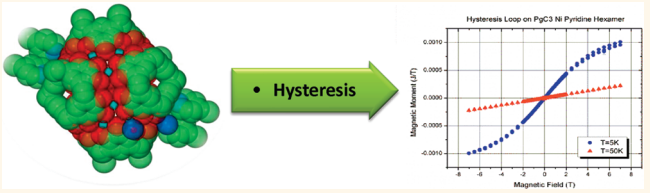

The magnetic behavior of nickel-seamed *C*-propylpyrogallol[4]arene dimeric and hexameric nanocapsular assemblies has been investigated in the solid state using a SQUID magnetometer. These dimeric and hexameric capsular entities show magnetic differentiation both in terms of moment per nanocapsule and potential antiferromagnetic interactions within individual nanocapsules. The weak antiferromagnetic behavior observed at low temperatures indicates dipolar interactions between neighboring nickel atoms; however, this effect is higher in the hexameric nickel-seamed assembly. The differences in magnetic behavior of dimer *versus* hexamer can be attributed to different coordination environments and metal arrangements in the two nanocapsular assemblies.

KEYWORDS: dimeric nickel-seamed nanocapsule · hexameric nickel-seamed nanocapsule · pyrogallol · soild-state magnetic behavior

Magnetically interesting transition metal-seamed architectures have been an active area of research for several years.[1−9] Transition metal oxide nanotubes/nanorings exhibit unique magnetic properties and have potential for biomagnetic applications, such as magnetic separation of lung cancer cells.[2] Likewise, manipulation of metallosupramolecular complexes has yielded tuned molecular magnetic materials, with possible application in information storage and data processing.[5,6] Another excellent example is the magnetically vectored nanocapsule that provides effective tumor penetration and controlled, switchable drug release *via* a remote RF field.[3,4]

Among supramolecular self-assembled architectures, transition metal-coordinated calixarenes, in particular with metals such as cobalt, nickel, manganese, and iron, have been explored with respect to magnetic anisotropy, antiferromagnetism, and superparamagnetism.[10−15] In striking contrast to the calix[4]arenes, the structurally related bowl-shaped polyphenolic pyrogallol[4]arene molecules are relatively unexplored with respect to their magnetic properties.[16] Pyrogallol[4]arene macrocyles self-assemble *via* hydrogen bonding into different geometric arrangements[17−19] including nanocapsules, nanotubes, and bilayers (Figure 1). As an addendum to hydrogen-bonded architectures, these macrocyles were made more robust by the insertion of metal ions in the framework.[16,17] Copper-seamed hexameric[20] and zinc-seamed dimeric[21] pyrogallol[4]arene nanocapsules were among the first reported metal-seamed organic nanocapsules (MONCs); however, magnetically interesting metals such as nickel and cobalt have been recently identified to also seam pyrogallol[4]arene nanocapsules.[16] Interestingly, under controlled conditions, the self-assembly process with copper and nickel atoms can be manipulated to yield either a dimer or a hexamer.[16,17,22]

The dimeric capsules are composed of two pyrogallol[4]arenes seamed together with eight metal centers across an equatorial belt, whereas the hexameric capsules are composed of six pyrogallol[4]arenes seamed together with 24 metal centers arranged in $(Metal)_3O_3$ arrays capping the face of a hypothetical octahedron.[20,21] Given the structural differences between the metal-seamed hexamers and dimers, we compared these MONCs magnetically not only to help identify appropriate guests, ligands, and linker R groups for building molecular devices, but also to yield important prototypes for exploring their magnetic behavior.[16]

Herein, we report the results of the first magnetic study on nickel-seamed

* Address correspondence to AtwoodJ@missouri.edu.

Received for review September 14, 2011 and accepted December 9, 2011.

Published online December 09, 2011
10.1021/nn203540e

C-propylpyrogallol[4]arene (PgC_3Ni) hexamers in powder form and compare the magnetic properties of the PgC_3Ni hexamers and dimers. This study affords magnetic differentiation between the penta-coordinated square pyramidal geometry of the nickel in the dimer with that of the octahedral geometry of the nickel in the hexamer. Although the magnetic moment of the Ni atoms does not vary significantly with the change in coordination environment, the environment does noticeably change the strength of the dipolar coupling.

Both the nickel-seamed hexameric and dimeric nanocapsules were prepared by combining 1 equiv of pyrogallol[4]arene with 4 equiv of nickel nitrate and 14 equiv of pyridine at controlled temperatures in methanol/DMSO. Synthesis at −40 °C yielded the PgC_3Ni hexamer while synthesis at the higher temperature of 50 °C yielded the PgC_3Ni dimer. The single crystal X-ray diffraction (XRD) results gave unit cell dimensions that matched previously acquired solid-state data.[22] In the current investigation, hysteresis curves and magnetic moment *versus* temperature SQUID magnetometer measurements were obtained for both the dimer and hexamer.

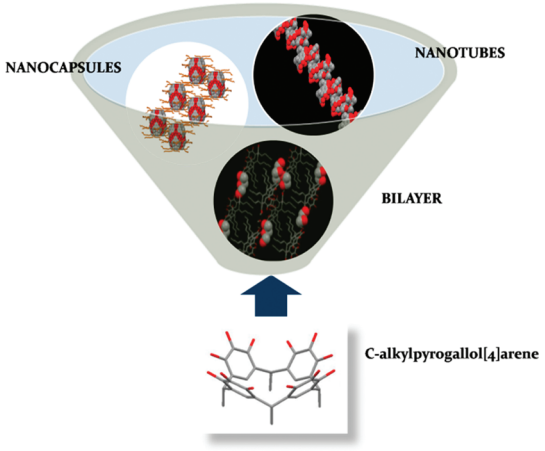

Figure 1. *C*-alkylpyrogallol[4]arene shown to self-assemble as a capsule, a tube, and a bilayer.

RESULTS AND DISCUSSION

The hysteresis curves at 5 K confirm the paramagnetic behavior of these MONCs in the solid state (Figure 2). The hysteresis data were fit to the quantum mechanical paramagnetic equation, assuming that $J = {}^1/_2$ and $g = 2$:

$$\mathbf{M} = Nm \tanh\left(\frac{gmJ\mu_0\mathbf{H}}{k_B T}\right) \quad (1)$$

Here, **M** is the total magnetic moment, **H** is the applied magnetic field, T is the temperature, N is the number of atoms in the sample, m is the magnetic moment per atom, k_B is Boltzmann's constant, g is the spectroscopic splitting factor, and J is the spin angular moment. The fit for the PgC_3Ni hexamer reveals (1.68 ± 0.01) μ_B per nickel atom, whereas the fit for the dimer reveals (1.65 ± 0.01) μ_B per nickel atom. Thus, the PgC_3Ni dimer and hexamer have nearly the same moment, which is surprising given the difference in the coordination environment of the metal atoms in the two structures.

To explore the possibility of magnetic interactions within and between MONCs, magnetic moment *versus* temperature measurements at 20 mT were performed on the powder samples of the PgC_3Ni hexamers and dimers (Figure 3). For both nanocapsules, we observe a deviation of the data from the Curie−Weiss law (eq 2) at low temperatures:

$$\mathbf{M} = \frac{A}{(T - T_{int})^{\gamma}} + C \quad (2)$$

Here, A and C are constants, T_{int} is the interaction temperature, and γ is the critical exponent which is set to 1. The deviation from an ideal noninteracting paramagnet takes the form of a negative interaction "temperature", indicating a weak antiferromagnetic interaction between the metal centers. The larger temperature value for the hexamer, (−2.2623 ± 0.0004) K, than for the dimer, (−1.0204 ± 0.0002) K, indicates that the interaction is stronger in the hexamer than the dimer. This behavior can be understood in the context

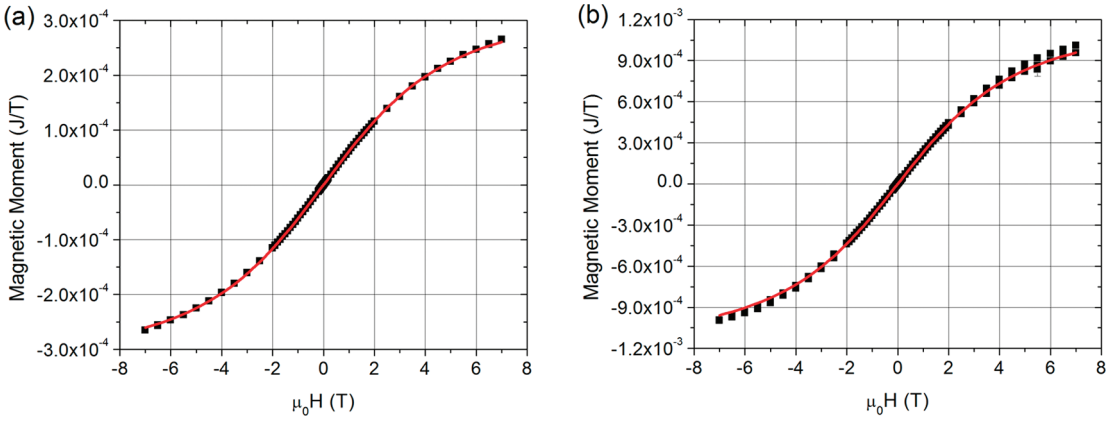

Figure 2. The 5 K hysteresis loop of powder samples of (a) *C*-propylpyrogallol[4]arene nickel hexamer and (b) *C*-propylpyrogallol[4]arene nickel dimer at 5 K. The red line is the fit to the data using eq 1. (All graphs include error bars.)

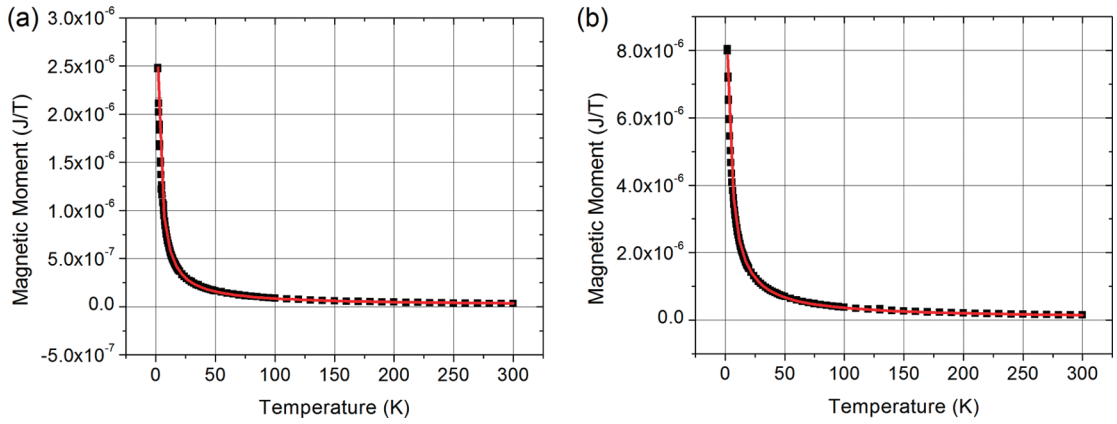

Figure 3. Magnetic moment *vs* temperature data at μ_0H = 20 mT of powder samples of (a) *C*-propylpyrogallol[4]arene nickel hexamer and (b) *C*-propylpyrogallol[4]arene nickel dimer. The red line is the fit to the data using eq 2. (All graphs include error bars.)

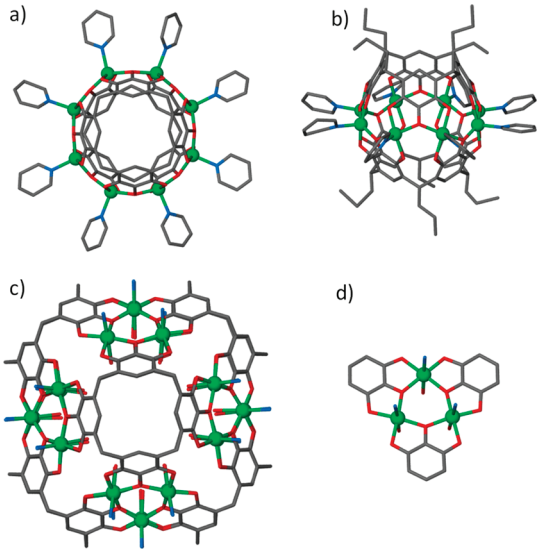

Figure 4. Structure determined by XRD of *C*-propylpyrogallol[4]arene nickel dimer shown from the (a) top and (b) side and structure determined by XRD of *C*-propylpyrogallol[4]arene nickel hexamer showing (c) the side view and (d) coordination environment. Green atoms are nickel atoms.

of the position of the metal atoms in the capsule frameworks.

In both capsules, the Ni atoms are close enough (~0.4 nm) that direct exchange is possible, but they are separated by oxygen atoms. Since the value of the magnetic moment per atom (in units of Bohr magnetons) is smaller than that of bulk Ni, direct exchange is unlikely. In addition, magnetostatic interactions are present. For the Ni dimer structure, all the Ni atoms lie in a single plane (Figure 4a,b). Therefore, energy minimization dictates that they will form flux closure structures at very low fields or have magnetostatic interactions with antiferromagnetic coupling. The latter is observed from the negative interaction temperature in the data. Since there are an even number of Ni atoms, pairs are formed, so frustration is not expected.

In contrast, for the Ni hexamer, the Ni atoms lie not within a single plane, but on the same curved surface (Figure 4c,d). Furthermore, the eight cyclic triads of $(Ni-O)_3$ in the hexamer result in an antiferromagnetic configuration as demonstrated by the negative interaction temperature. However, although this antiferromagnetic configuration is stable between two adjacent metal−oxygen centers, the third Ni atom may be frustrated in its spin direction. This unsymmetrical alignment of the magnetic moments of the frustrated metal centers in the hexamers could account for the stronger antiferromagnetic interaction of the PgC_3Ni hexamers as compared to the PgC_3Ni dimers.

Finally, there is no evidence of interactions between adjacent MONCs in the hysteresis loops given the complete overlap of the virgin curve with the major loops, even at 5 K. Furthermore, this lack of plausible evidence for interactions is not dependent upon the phase of the material—either solution (data not shown) or powder—and is likely due to the small magnitude of the observed net magnetic moments. Therefore, the only observed interactions are Ni atom to Ni atom within a single MONC.

The results for the nickel-seamed dimers are in agreement with our earlier X_mT product *versus* T measurements and density functional theory (DFT) and complete active space self-consistent field (CASSCF) calculations.[16] The change in X_mT value with respect to temperature indicates weak antiferromagnetic exchange between the nickel atoms. The computations on the $Ni(catechol)_2(pyridine)$ model complexes suggest that each individual nickel center has a triplet state but the X_mT product *versus* T data demonstrate that the dimer is diamagnetic overall. In addition, the experimental data are consistent with a simple 1*J*-model in which all eight metal ions are equivalent.[16]

CONCLUSION

In summary, we have studied the solid-state magnetic behavior of two different nanocapsular assemblies of nickel-seamed *C*-propylpyrogallol[4]arene. These dimeric and hexameric nanocapsules have similar magnetic moments but different interaction temperatures. The negative interaction temperatures at 5 K indicate a weak antiferromagnetic dipolar interaction. These antiferromagnetic interactions are more pronounced in the nickel-seamed hexamer due to the positioning of the metal centers in triads along a curved surface in contrast to the equatorial arrangement of the metal centers in the dimer. Our studies in this area continue with new magnetically interesting metal-seamed architectures with a view toward exploring and controlling the magnetic behavior for desired functionality. The judicious choice of the metals, ligands, and R groups should allow us to not only control the architecture and magnetic behavior of the nanocapsules but also introduce MONCs suitable for nanowires and spintronics applications. In addition, the magnetic properties of these MONCs may be useful in contrast agents for magnetic resonance energy or tagging agents for biomedical assays.

METHODS

The nickel-seamed dimer and hexamer were synthesized using literature procedures.[22] In a general experiment, a methanolic solution of pyrogallol[4]arene (1 equiv) was added to a methanolic solution of nickel nitrate (4 equiv) and pyridine (14 equiv). For both dimer and hexamer, standing over a number of hours afforded crystals suitable for single X-ray diffraction measurements. These crystalline samples were utilized for magnetic measurements.

Acknowledgment. We thank NSF for support of this research (J.L.A.). This work was supported by the National Science Foundation (NSF) and National Institute for Standards and Technology (NIST). It utilized facilities supported in part by the NSF under Agreement No. DMR-0944772 (C.L.D.). The use of specific trade names does not imply endorsement of products or companies by NIST, but they are used to fully describe the experimental procedures.

REFERENCES AND NOTES

1. Akutagawa, T.; Nishihara, S.; Takamatsu, N.; Hasegawa, T.; Nakamura, T.; Inabe, T. Co^{2+}(15-Crown-5) Magnetic Supramolecular Cation in $[Ni(Dmit)_2]$-Π-Spin System. *J. Phys. Chem.* **2000**, *104*, 5871–5873.
2. Fan, H.-M.; Yi, J.-B.; Yang, Y.; Kho, K.-W.; Tan, H.-R.; Shen, Z.-X.; Ding, J.; Sun, X.-W.; Olivo, M. C.; Feng, Y.-P. Single-Crystalline Mfe(2)O(4) Nanotubes/Nanorings Synthesized by Thermal Transformation Process for Biological Applications. *ACS Nano* **2009**, *3*, 2798–2808.
3. Kong, S. D.; Zhang, W.; Lee, J. H.; Brammer, K.; Lal, R.; Karin, M.; Jin, S. Magnetically Vectored Nanocapsules for Tumor Penetration and Remotely Switchable on-Demand Drug Release. *Nano Lett.* **2010**, *10*, 5088–5092.
4. Li, G.-p.; Wang, Y.-x.; Zhang, Y.-f.; Zhang, C.-f. Anti-Tumor Effect in Vitro of ^{188}re Labeled Herceptin-Coated Magnetite Nanoparticles. *Zhonghua Heyixue Zazhi* **2007**, *27*, 16–18.
5. Pardo, E.; Ruiz-Garcia, R.; Cano, J.; Ottenwaelder, X.; Lescouezec, R.; Journaux, Y.; Lloret, F.; Julve, M. Ligand Design for Multidimensional Magnetic Materials: A Metallo-Supramolecular Perspective. *Dalton Trans.* **2008**, 2780–2805.
6. del Carmen Giménez-López, M.; Moro, F.; La Torre, A.; Gómez-García, C. J.; Brown, P. D.; van Slageren, J.; Khlobystov, A. N. Encapsulation of Single-Molecule Magnets in Carbon Nanotubes. *Nat. Commun.* **2011**, *2*, 407.
7. Waldmann, O.; Hassmann, J.; Müller, P.; Volkmer, D.; Schubert, U. S.; Lehn, J. M. Magnetism of Self-Assembled Mono- and Tetranuclear Supramolecular Ni^{2+} Complexes. *Phys. Rev. B* **1998**, *58*, 3277–3285.
8. Waldmann, O.; Hassmann, J.; Koch, R.; Mueller, P.; Hanan, G. S.; Volkmer, D.; Schubert, U. S.; Lehn, J. M. *Mater. Res. Soc. Symp. Proc.* **1997**, *488*, 841–846.
9. Waldmann, O.; Hassmann, J.; Müller, P.; Hanan, G. S.; Volkmer, D.; Schubert, U. S.; Lehn, J. M. Intramolecular Antiferromagnetic Coupling in Supramolecular Grid Structures with Co^{2+} Metal Centers. *Phys. Rev. Lett.* **1997**, *78*, 3390–3393.
10. Petit, S.; Pilet, G.; Luneau, D.; Chibotaru, L. F.; Ungur, L. A Dinuclear Cobalt(II) Complex of Calix[8]arenes Exhibiting Strong Magnetic Anisotropy. *Dalton Trans.* **2007**, 4582–4588.
11. Ali, A.; Joseph, R.; Mahieu, B.; Rao, C. P. Synthesis and Characterization of a (1 + 1) Cyclic Schiff Base of a Lower Rim 1,3-Derivative of *p-tert*-Butylcalix[4]arene and Its Complexes of VO^{2+}, UO_2^{2+}, Fe^{3+}, Ni^{2+}, Cu^{2+} and Zn^{2+}. *Polyhedron* **2010**, *29*, 1035–1040.
12. Bi, Y.; Liao, W.; Xu, G.; Deng, R.; Wang, M.; Wu, Z.; Gao, S.; Zhang, H. Three *p-tert*-Butylthiacalix[4]Arene-Supported Cobalt Compounds Obtained in One Pot Involving *in Situ* Formation of N_6H_2 Ligand. *Inorg. Chem.* **2010**, *49*, 7735–7740.
13. Bi, Y.; Wang, X.-T.; Wang, B.-W.; Liao, W.; Wang, X.; Zhang, H.; Gao, S.; Li, D. Two $Mn(II)_2Ln(III)_4$ (Ln = Gd, Eu) Hexanuclear Compounds of *p-tert*-Butylsulfinylcalix[4]arene. *Dalton Trans.* **2009**, 2250–2254.
14. Kennedy, S.; Karotsis, G.; Beavers, C. M.; Teat, S. J.; Brechin, E. K.; Dalgarno, S. J. Metal−Organic Calixarene Nanotubes. *Angew. Chem.* **2010**, *49*), S4205/4201–S4205/4205.
15. Pietraszkiewicz, M. Calixarenes as Ligands for Transition Metals, Actinides and Lanthanides. *Wiad. Chem.* **1998**, 69–89.
16. Atwood, J. L.; Brechin, E. K.; Dalgarno, S. J.; Inglis, R.; Jones, L. F.; Mossine, A.; Paterson, M. J.; Power, N. P.; Teat, S. J. Magnetism in Metal−Organic Capsules. *Chem. Commun.* **2010**, *46*, 3484–3486.
17. Dalgarno, S. J.; Power, N. P.; Atwood, J. L. Metallo−Supramolecular Capsules. *Coord. Chem. Rev.* **2008**, *252*, 825–841.
18. Dalgarno, S. J.; Cave, G. W. V.; Atwood, J. L. Toward the Isolation of Functional Organic Nanotubes. *Angew. Chem.* **2006**, *45*, 570–574.
19. Dalgarno, S. J.; Antesberger, J.; McKinlay, R. M.; Atwood, J. L. Water as a Building Block in Solid-State Acetonitrile−Pyrogallol[4]arene Assemblies: Structural Investigations. *Chem.—Eur. J.* **2007**, *13*, 8248–8255.
20. McKinlay, R. M.; Cave, G. W. V.; Atwood, J. L. Supramolecular Blueprint Approach to Metal-Coordinated Capsules. *Proc. Natl. Acad. Sci.* **2005**, *102*, 5944–5948.
21. Dalgarno, S. J.; Power, N. P.; Warren, J. E.; Atwood, J. L. Rapid Formation of Metal-Organic Nanocapsules Gives New Insight into the Self-Assembly Process. *Chem. Commun.* **2008**, 1539–1541.
22. Kumari, H.; Mossine, A. V.; Kline, S. R.; Dennis, C. L.; Fowler, D. A.; Barnes, C. L.; Teat, S. J.; Deakyne, C. A.; Atwood, J. L. Controlling the Self-Assembly of Metal-Seamed Organic Nanocapsules *Angew. Chem.* **2011**, In press, DOI: anie.201107182.